




## Article

# Frequency Stability Evaluation in Low Inertia Systems Utilizing Smart Hierarchical Controllers

Minas Patsalides <sup>1,\*</sup> , Christina N. Papadimitriou <sup>1</sup>, Venizelos Efthymiou <sup>1</sup>, Roberto Ciavarella <sup>2</sup>, Marialaura Di Somma <sup>3</sup> , Anna Wakszyńska <sup>4</sup>, Michał Kosmecki <sup>4</sup> , Giorgio Graditi <sup>3</sup> and Maria Valenti <sup>3</sup>

<sup>1</sup> FOSS Research Centre for Sustainable Energy, University of Cyprus, 1678 Nicosia, Cyprus; papadimitriou.n.christina@ucy.ac.cy (C.N.P.); efthymiou.venizelos@ucy.ac.cy (V.E.)

<sup>2</sup> ENEA–Energy Technologies Department, 00196 Rome, Italy; roberto.ciavarella@enea.it

<sup>3</sup> ENEA–Energy Technologies Department, 80055 Portici (Naples), Italy; marialaura.disomma@enea.it (M.D.S.); giorgio.graditi@enea.it (G.G.); maria.valenti@enea.it (M.V.)

<sup>4</sup> Department of Automation and System Analysis, Institute of Power Engineering (IEn) Gdańsk Division, PL80-870 Gdańsk, Poland; a.wakszynska@ien.gda.pl (A.W.); m.kosmecki@ien.gda.pl (M.K.)

\* Correspondence: patsalides.minas@ucy.ac.cy

Received: 8 May 2020; Accepted: 29 June 2020; Published: 7 July 2020



**Abstract:** The high penetration of the Renewable Energy Sources and other emerging technologies likely to be installed in future power grids will pose new operational challenges to grid operators. One of the main issues expected to affect the operation of the power grid is the impact of inverter-based technologies to the power system inertia and, hence, to system stability. Consequently, the main challenge of the future grid is the evaluation of the frequency stability in the presence of inverter-based systems and how the aforementioned technology can support frequency stability without the help of the rotating masses of the traditional power grid systems. To assess the above problem, this paper proposes a methodology to evaluate the frequency stability in a projection of the real distribution grid in Cyprus with the time horizon to be the year 2030. The power grid under investigation is evaluated with and without the presence of smart hierarchical controllers for providing support to the power system under disturbance conditions. The advanced controllers were applied to manage the available power resource in a fast and effective manner to maintain frequency within nominal levels. The controllers have been implemented in two hierarchical levels revealing useful responses for managing low-inertia networks. The first is set to act locally within a preselected area and the second level effectively supporting the different areas for optimal operation. After undertaking a significant number of simulations for time-series of one year, it was concluded from the results that the local control approach manages to minimize the frequency excursion effectively and influence all related attributes including the rate of change of frequency (RoCoF), frequency nadir and frequency zenith.

**Keywords:** frequency controller; frequency stability; low inertia; distributed energy resources; disturbance conditions

## 1. Introduction

### 1.1. Motivation

In a power system, the first few seconds after a disturbance are crucial for maintaining the frequency within the acceptable range and hence ensuring that the power system will remain stable. The figure below shows the frequency regulation process established by ENTSO-E and presents how the traditional systems are expected to deal with the under-frequency events within the depicted timeframe [1].

In Figure 1, it is noticeable that the system's inertial response is critical in conventional power systems since it is the first and the fastest system's response to contain potential instability problems and is responsible for limiting rate of change of frequency, allowing slower hierarchical frequency support and generation rescheduling that follows to support the frequency and its restoration to the nominal value.

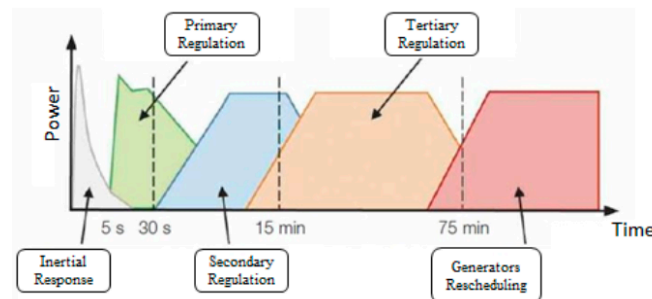


**Figure 1.** The frequency regulation process steps and timeframe [1].

As power systems evolve and synchronous units are being replaced by inverter-based technologies, i.e., Renewable Energy Sources (RES) and storage, the overall system inertia and frequency control capabilities lowers. Moreover, this often leads to more decentralized systems with a large amount of small generating units, which can be problematic for managing in a centralized manner. Based on this, new challenges related to the system stability and robustness [2] are expected to appear and need to be addressed by the system operators, as inverter-based technologies are expanding rapidly within current power grids due to regulations/initiatives for environment protection imposed by governments worldwide. Consequently, for optimal handling of frequency stability and achieving the desirable balance between consumption and power production after a disturbance, enhancing the system frequency in that way, it is mandatory to adopt intelligent and advanced frequency control schemes that can act automatically and in the decentralized manner, utilizing inverter-connected generator capabilities to support system stability.

### 1.2. Literature Review

For the above reasons, the impact of distributed inertia-less power sources on the frequency regulation has received increasing research interest during the last decade.

In the literature, several efforts have been devoted to analyzing the effects of the high penetration of RES on grid frequency control and different approaches have been presented on how stability of the system can be ensured and secured.

The authors in [3] explore the interactions between inertia, Fast Frequency Response (FFR), governor response, and UFLS. It also stresses the necessity for new operational practices and policies, as well as novel market structures and mechanisms for accounting non-synchronous generation into frequency control. The authors in [4] investigate the supplementary inertia technologies that could be deployed to mitigate RoCoF. The technologies considered include Frequency Trigger Response (FTR), RoCoF triggered response, Time Triggered Response (TTR), Droop Response (DR), Step and Droop Response and Stepped response with variable ramp rates. In [5], a combination of synthetic inertia (SI) and governor control provided by wind and PV power plants was presented to show how frequency control can be implemented in bulk power systems. In [6], three different control strategies of the Li-ion based ESS for providing Primary Frequency Regulation (PFR) have been analyzed and compared. Additionally, in both [7,8] storage has been utilized for frequency support. FFR and Enhanced FFR have been investigated in [9]. Furthermore, [10] discusses FFR concepts, types of FFR and illustrates its impact on bulk power system while [11] explores opportunities and possible roles for FFR in future power systems. In several papers [12–15], hierarchical, distributed approaches to achieving stability, such as voltage or small and large signal stability, and dealing with harmonics in hybrid microgrids

with nonlinear and unbalanced loads, have been investigated. The authors in [12] propose controllers based on sliding mode control and Lapunov function theory, while [13] adds additional controller based on fractional-sliding mode control. The authors in [14] introduce a new virtual impedance scheme and presents power calculation method, using neural networks to solve harmonic power flow, and [15] presents a mixed  $H_2/H_\infty$  control strategy, based on multi-objective optimization and fuzzy decision making, for setpoint tracking and disturbance rejection, additionally improving the fault ride through capabilities of microgrids.

### 1.3. Contribution and Paper Structure

The main contribution of this work is to present a methodology for evaluating frequency stability of a future grid, using a model based on a real Cypriot power network, with high RES and storage penetration, considering the future pan-European grid power scenario. In the proposed solution, local problems are resolved locally through a hierarchical control function for network operational planning purposes that offer fast frequency restoration control. Therefore, the added value of this paper is evaluating the contribution of inertia-less resources in the effective restoration of frequency, using a complex grid Cyprus grid model consisting of both transmission and distribution level, while reporting possible disadvantages or problems leading to the need for alternative frequency control methods. Moreover, in contrast to most cases studied in the literature, the proposed solution is designed as an “operation tool”, allowing for evaluating grid conditions during whole day, in an interval for which time series data are available.

The paper is structured as follows. Section 2 presents the case study of the future projected grid along with the methodology of the frequency evaluation and the proposed hierarchical control. Section 3 presents the Simulation Results when applying the methodology in a part of the Cyprus grid as it will be projected in the future. Discussion, along with conclusions, provide the general outcomes of the work undertaken in the paper and can be found in Sections 4 and 5, respectively.

## 2. Case Study—Methodology

### 2.1. Grid System Under Investigation

The considered electricity grid system is originating from both the Cyprus transmission and distribution grid available at Electricity Authority Cyprus (EAC). The grid system under investigation models a part of the real physical grid area of Cyprus in 2019. Specifically, the model represents a synthetic benchmark grid which comprises of transmission substations with terminals of 132 kV voltage level. Additionally, it comprises of distribution substations operating at voltage levels of 11 kV and 400 V phase to phase.

The model contains a total of 1721 lines, 3009 busbars (4891 terminals), 1006 transformers, 1925 loads (including 962 electric vehicle loads), and 1931 generators (962 PV systems, 2 Synchronous machines, 962 battery energy storage systems, 2 Hydro systems, 2 Wind Farm systems and 1 biomass unit). In addition, it provides 2284 protection devices (993 fuses) and 1291 breakers/switches.

In more detail, the Cyprus grid model includes the distribution network of three transmission substations of Cyprus: ALAMBRA—Area1, PROTARAS—Area 2 and DISTRICT OFFICE—Area 3. Each transmission substation constitutes a different control area with distributed generation, storage, electric vehicles, and loads. Figure 2 presents a part of the ALAMBRA distribution network which includes the transmission substation (marked with S symbol) and a distribution substation. The model of the distribution substation is shown in Figure 3. The distribution system of Cyprus has a radial architecture and the transmission system a ring architecture and exactly a replica of this is the proposed power system under investigation. The backbone of the power grid in Cyprus is operating at 132 kV nominal voltage and it is designed following the n-1 design criterion to offer added security of supply. The distribution grid is using two operating nominal voltages, 11 and 22 kV. The low-voltage system is operating with the nominal voltage of 400/230 V using an overhead or underground grid depending

on proximity to the living environment. Distribution substations are using standardized designs based on ground mounted substations ranging from 300 to 1000 kVA capacity and pole mounted ranging from a 25 to 200 kVA capacity. Design details are based on the respective European standards using effectively earthed systems.

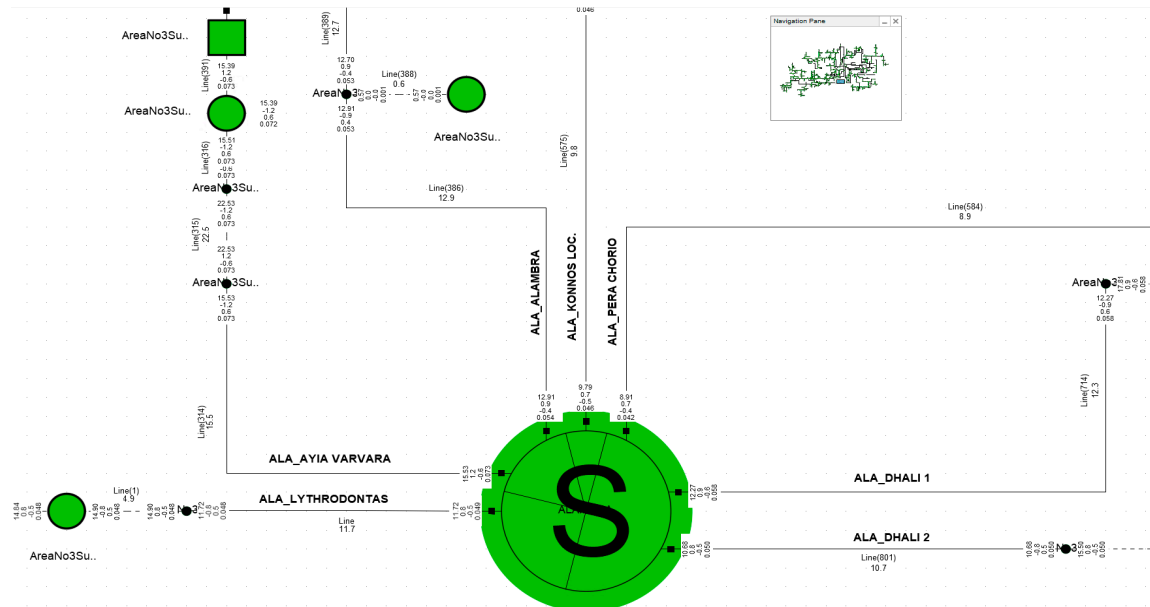


**Figure 2.** Transmission Substation and Distribution Substation models for ALAMBRA distribution network.

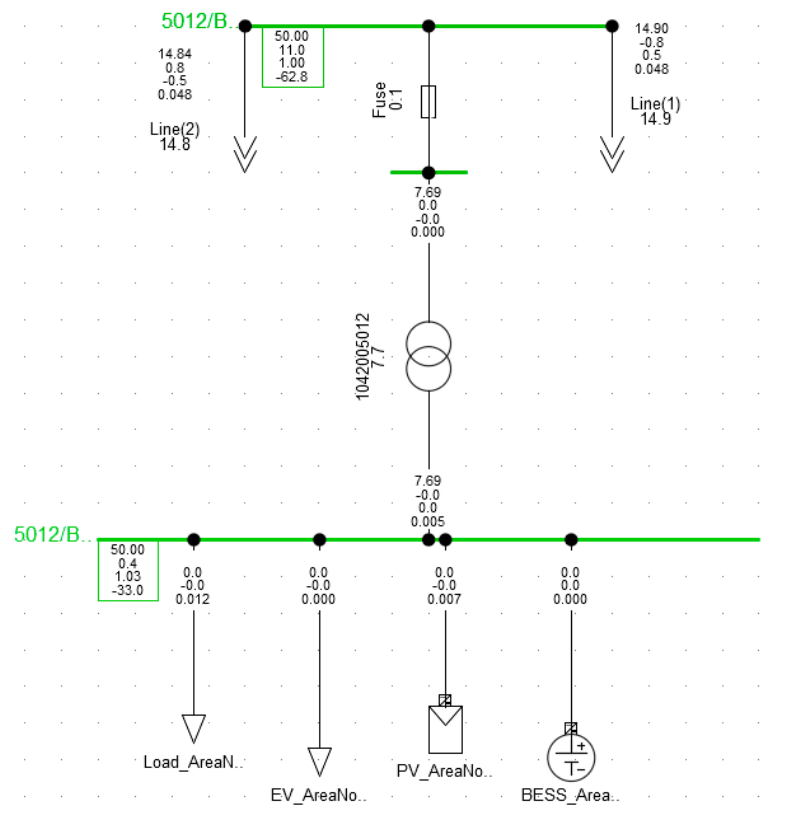


**Figure 3.** Composition of Distribution Substation model.

The distribution substation model is composed of a distribution transformer and aggregated elements for load, electric vehicles, photovoltaic systems, and storage units. The main grid model also incorporates a conventional power generation and a wind power generation area shown in Figures 4 and 5, respectively. The wind power generation area is composed of two transmission transformers and two aggregated areas of wind turbines. The conventional power generation area includes two transmission transformers and two synchronous machines.

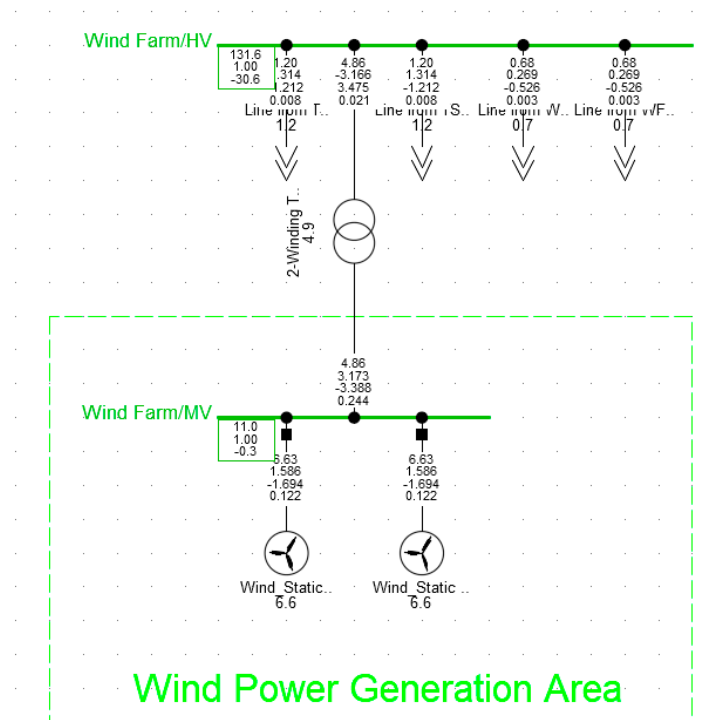


Figure 4. Model of Wind Power Generation Area.

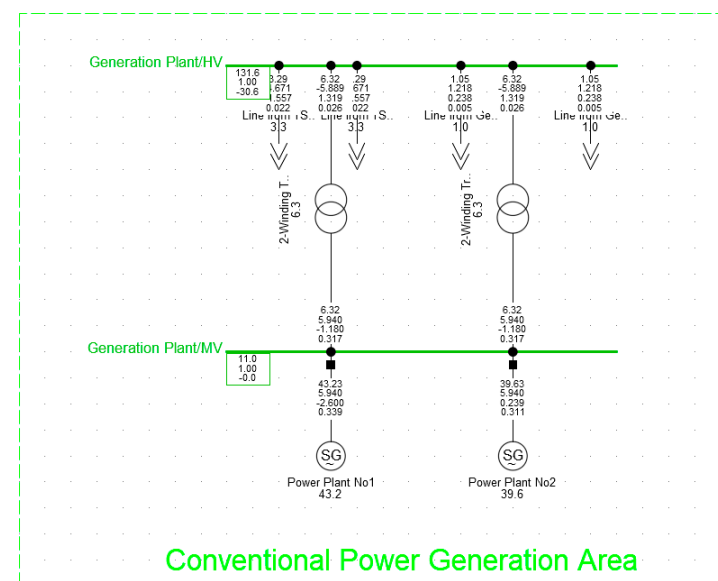


Figure 5. Model of Conventional Power Generation Area.

## 2.2. Scenario

In this selected scenario, a European agreement for climate mitigation is achieved and fossil fuel consumption is expected to be low worldwide by the year 2030. Therefore, due to the low dependence on conventional fuels, fuel costs are relatively low. The CO<sub>2</sub> costs are high due to the existence of a global carbon market. The EU's ambition for Greenhouse Gas (GHG) emission reductions is achieved through this selected scenario, an 80–95% GHG reduction. The strategy focuses on the deployment of large-scale RES technologies [16].

Large-scale RES deployment is accompanied by centralized storage solutions such as pumped hydro storage, compressed air, etc. Electrification of transport, heating and industry can be supported by both centralized (large-scale) and decentralized (domestic) storage solutions. However, the political focus is mainly on the supply side so it is expected that large amount of fossil-free generation will be incentivized for investments in energy efficiency.

The scenario's production per power source is shown in Table 1. It shall be noted that in the case of evaluating the stability behavior of the Cyprus power grid while investigating a realistic case scenario, it will be required to omit hydro power generation and reallocate its power potential to the rest of the generation technologies based on the roadmap of Cyprus power production energy mix [17].

**Table 1.** Scenario case for 2030—Nominal Power Production per type.

Scenario—Nominal Capacity Per Power Source Type (MVA)						
Scenario Cases	Solar	Wind	Hydro	Biomass	Conventional	Pump Storage
2030	42.3	42.3	48.9	9.2	22.5	—

In this work, four power events were defined (Table 2) to enable the study of frequency stability. The specific events simulate realistic conditions and challenges that the grid operator may confront. The stability analysis scenario adopted for 2030 simulates the loss of generation capacity of one power source.

**Table 2.** Power Events under investigation for 2030 Scenario.

Stability Analysis Scenarios for 2030—Loss of Power Generation (Affected Source Type Marked with Bold Style)				
Source Type	Fault in Area 1	Fault in Area 2	Fault in Wind Station	Fault in Gen. Station
Solar	<b>42.3</b>	<b>42.3</b>	42.3	42.3
Wind	42.3	42.3	<b>42.3</b>	42.3
Hydro	<b>34.2</b>	34.2	34.2	34.2
Biomass	6.4	<b>6.4</b>	6.4	6.4
Conventional	15.8	15.8	15.8	<b>15.8</b>

## 2.3. Control Scheme

High rate RES penetration along with the electrification of other carriers such as heating and transport, and the exploitation of flexibility resources at distribution level, will cause number of network operation issues. Under this prism, the frequency of the future system will no longer be centrally managed under the responsibility of Transmission System Operators (TSOs).

To deal with this challenge, a radically new approach is required. Innovative monitoring systems based on a fully instrumented network, and dynamic autonomous distributed control functions should be employed to collect detailed local information, from all low- and medium-voltage networks to the high voltage system operators. This will allow operators to detect local problems and establish a secure and optimal reserves activation action using distributed (flexible) resources [18].

Therefore, under the transformation of the grid, a real transition towards a new functional decentralized control architecture is also needed. Under this decentralized control architecture,

local problems are solved locally by using local controllers to decide on corrective actions for local issues.

The adopted controller aims to solve the power grid frequency instability issues using the distributed resources present in the grid. The specific controller has been developed and presented in [19,20] and for the purpose of this work, it has been adapted accordingly in order to be incorporated in each control area (implementing a hierarchical approach), which is defined in the grid with the aim to solve local problems in a local way. Furthermore, if an instability event occurs in area 1 only, storage systems in the control area 1 will be involved in the frequency stability process.

In Figure 6, the control logical scheme is shown with the main functions highlighted.

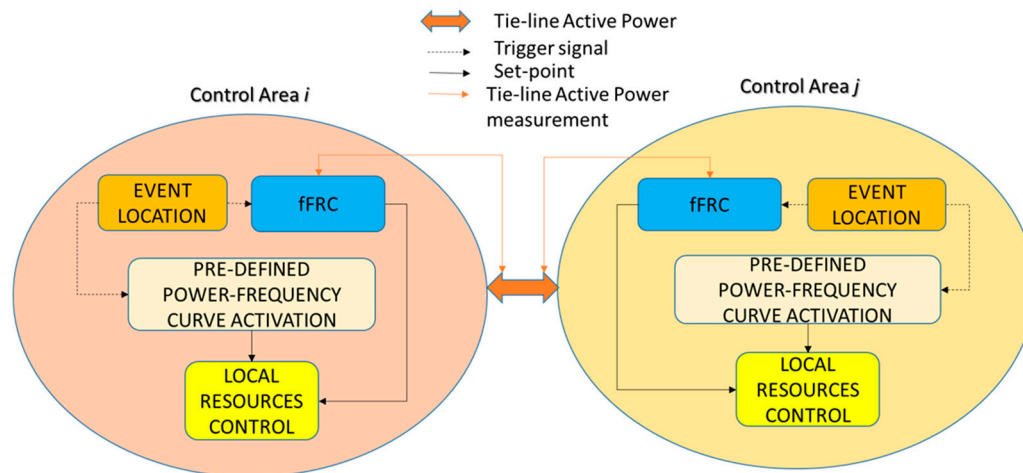


Figure 6. Control logic scheme.

The main local controller functions are:

- Event Location;
- fFRC—fast Frequency Restoration Control;
- Pre-defined Power–Frequency curve calculation;
- Local Resources Control;

The figure below shows the control area level with highlighted the main functions and their interconnections.

It is also possible to observe in Figure 7, the “SecControl” and “AGCCControl” functions that represent respectively a secondary control and the traditional Automatic Gain Control. For the purposes of this work, these functions have been deactivated but their presence gives more flexibility to the controller for future applications.

Finally, in the Control Area level the “dpBorder” function can also be active. It evaluates the total tie-lines active power variation and communicates the obtained result to “fFRC” and “Event Location” functions.

The “Event location” function locates the possible instability event. For this purpose, the frequency and total active power tie-lines variation signs among the near control areas are evaluated. The instability event is external to the area if the signs are concordant, internal to it in case of discordant signs. In case of internal instability, a trigger signal activates both the fFRC function and power–frequency pre-defined response of the resources at local resources level. The fFRC, in particular, deals with the total tie lines’ active power variation with the aim to counteract it using the assets in the own control area while the power–frequency curve predefined is calculated for power resources at control area level considering the available active power flexibility.

Figure 8 shows the communication interface that allows the interaction between control area level and local resources level.



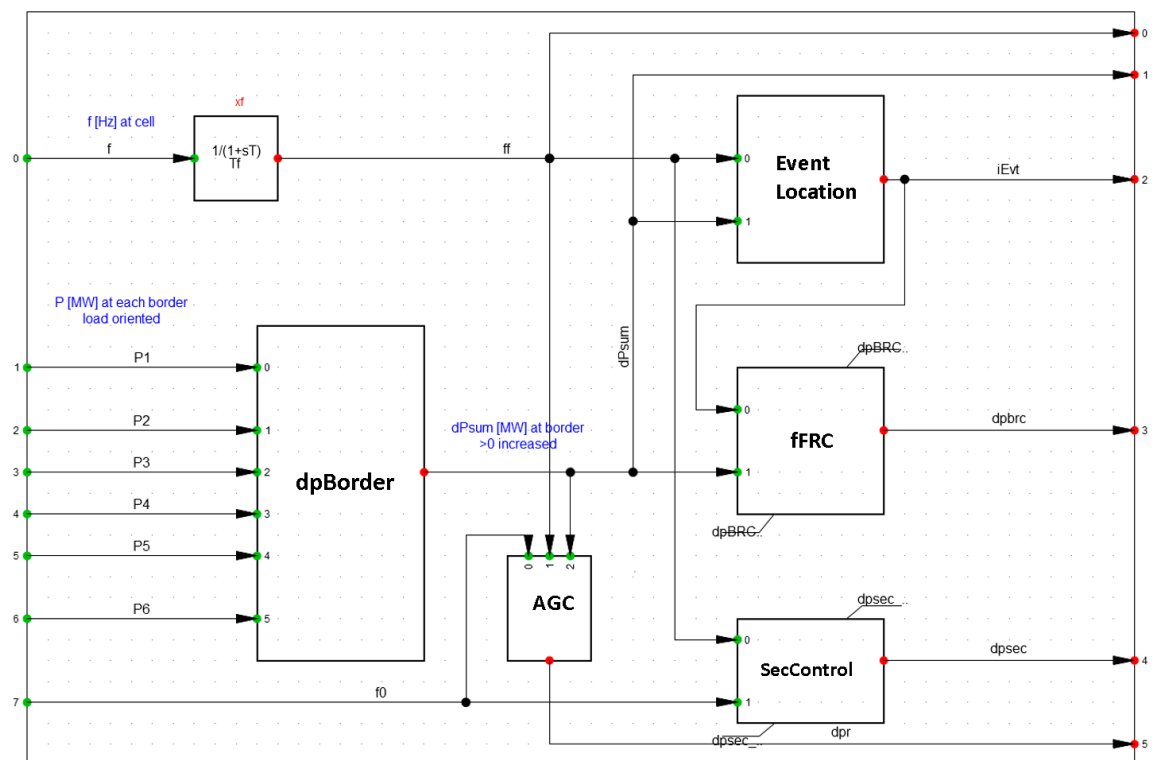


Figure 7. Functions and Interconnections of area controller.

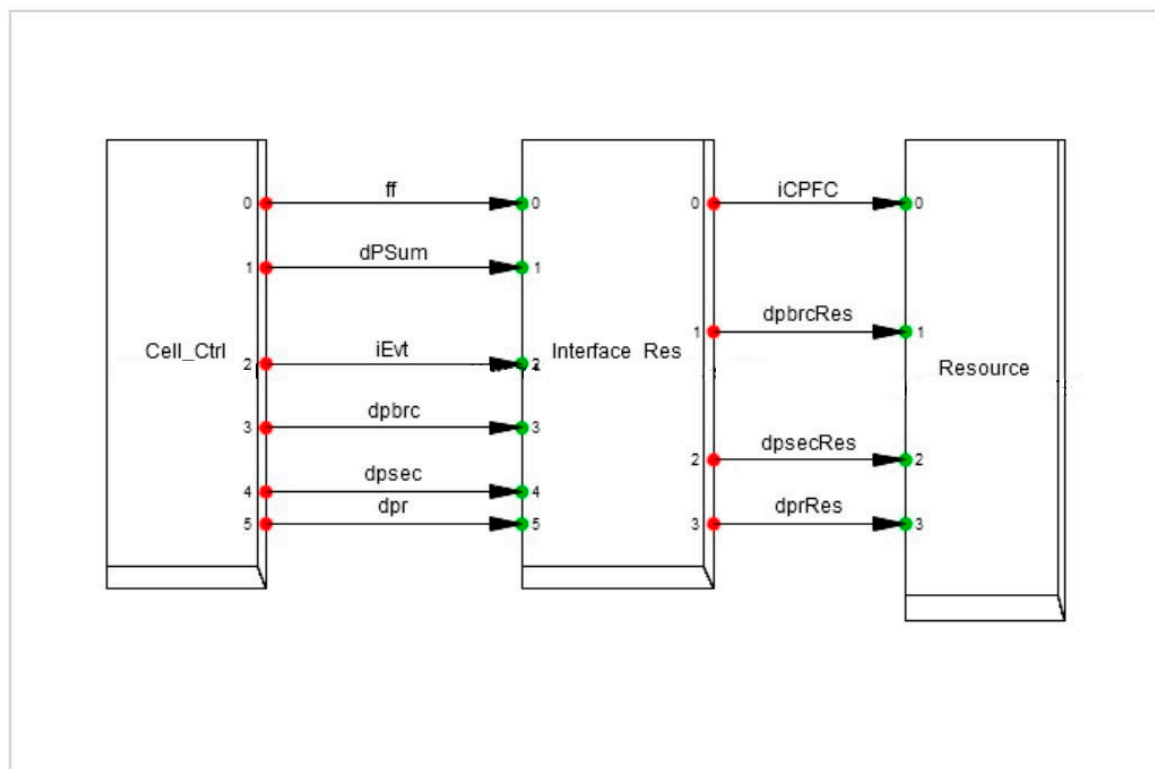


Figure 8. Communication Interface Level.



Figure 9 shows the “Interface Res” details.

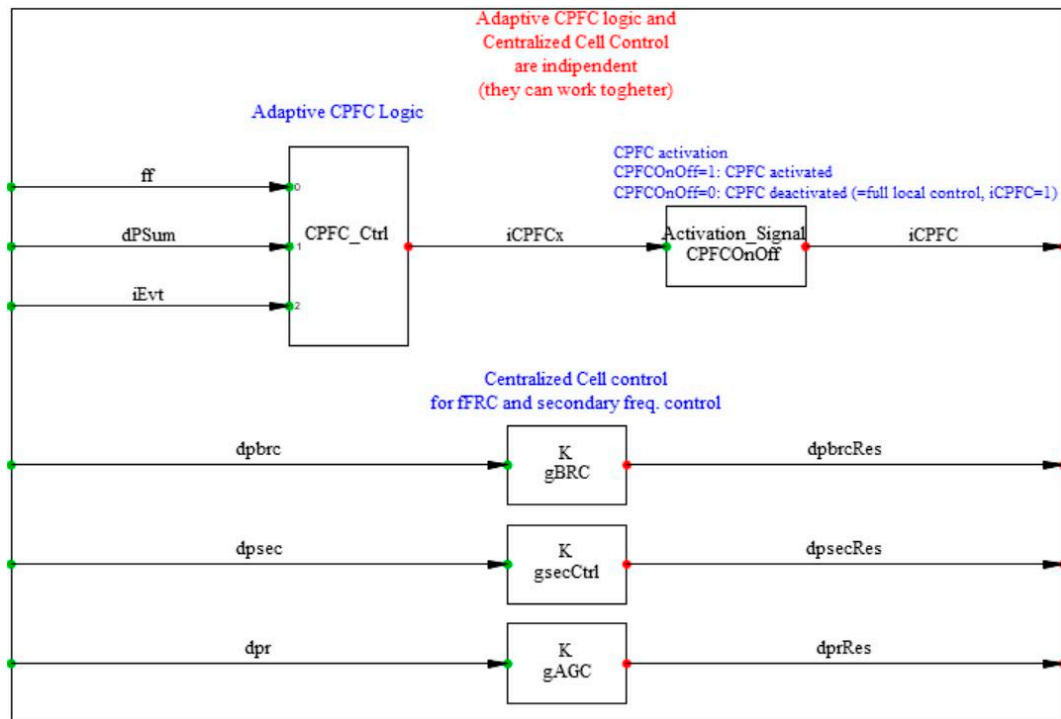


Figure 9. Interface\_Res level.

The “CPFC\_Ctrl” function in the figure enables the local resource response in case an instability event is detected internal to the control area. Its output iCPFC is a trigger for the pre-defined curve activation, as shown in Figure 10.

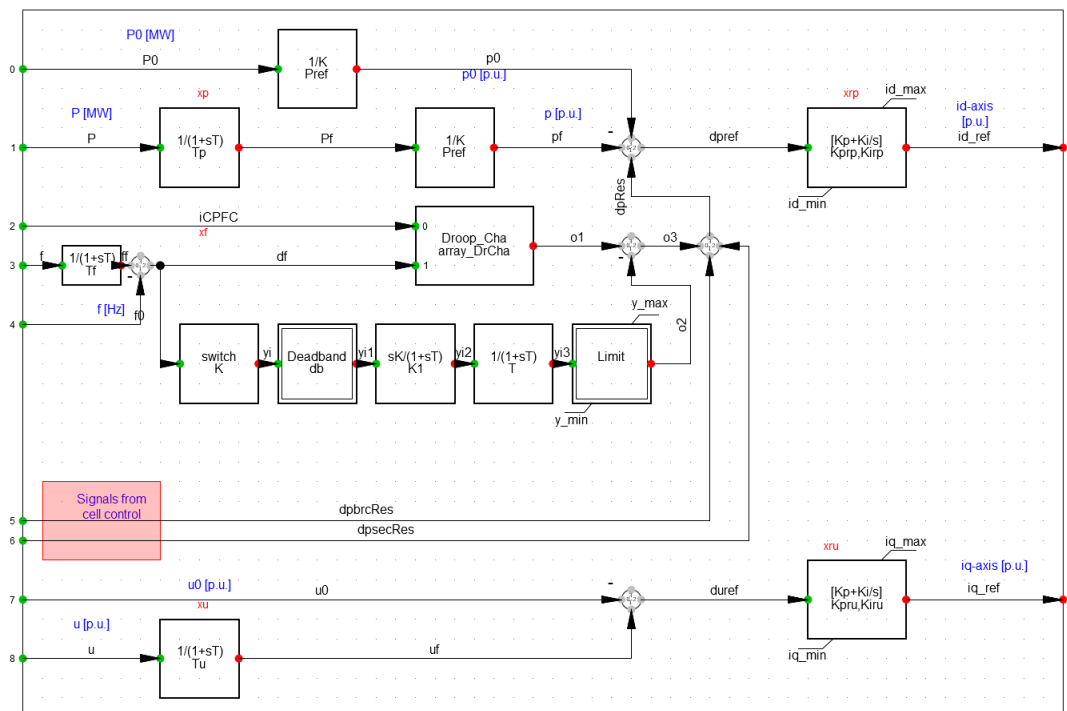


Figure 10. Local Resources Control.

The function “Droop\_Cha” represents the Pre-defined Power-Frequency function. The Power-Frequency curve is calculated per each control area base using the following steps:

1. Active power flexibility evaluation per each asset in the control area. The information is stored in a merit order collection table (MOC) containing the values about  $P_{max}$  (W),  $P_{min}$  (W),  $P_{actual}$  (W),  $P_{reserve}$  (W) per each asset in the control area. The values in the table represent, respectively, the max and min power limits of the asset, the measured actual power and finally Preserve represent the available flexibility. The information is sorted in descending order based on  $P_{reserve}$  values;
2. Control area's contribution to Frequency containment CPFC (W/Hz);
3. Frequency error threshold definition  $f_{error}$  (Hz);
4. Frequency threshold steps definition  $n_{step}$ ;
5. Calculation of the  $\Delta f_{step} = \frac{f_{error}}{n_{step}}$ ;
6. Calculation of the total active power contribution per each step:  $P_{step} = CPFC \times \Delta f_{step}$
7. Active power contribution provided by assets for negative and positive frequency slope.

Regarding the last point mentioned, the flowchart below (Figure 11) shows the method to calculate the active power contribution by each asset in the control area for the negative frequency slope.

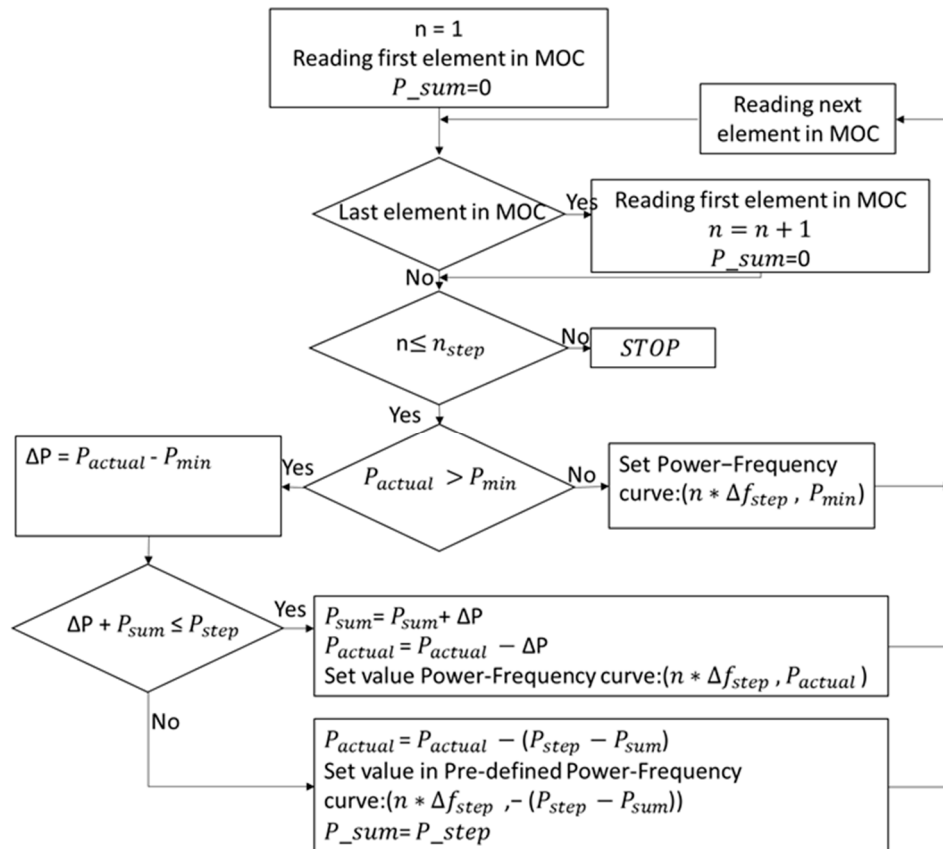


Figure 11. Flowchart for calculating active power contribution.

The active power contribution for the positive frequency slope can be obtained easily starting from the above flow chart. It is worth noting that the pre-defined power-frequency curve is dependent by  $n_{step}$ ,  $f_{error}$ , CPFC and assets active power flexibility.

The proposed control aims to contain the frequency deviation in a fast way without considering the lower inertia effects. A possible improvement could be integrating the proposed control with a synthetic inertia control which will be investigated through planned future work.

## 2.4. Methodology

After setting up the simulation scenario based on Section 2.2, multiple simulations were performed with and without controllers responsible for restoring frequency close to the nominal value. The results are evaluated based on the key performance indices (KPIs) shown in Table 3. The adopted KPIs are used in the simulation phase to prove the effectiveness of the proposed control scheme. Indeed, the KPIs used in the paper are among the most widely used indicators to assess the stability performance of power system in the presence of high RES penetration. RoCoF and NADIR are the most widely used indicators in the literature to assess the frequency performance in the frequency containment period [21–23]. RoCoF measures the frequency gradient after an active power imbalance. On the other hand, the NADIR indicator corresponds to the lowest frequency value obtained after a power imbalance, which depends on the system inertia, the response of the available frequency containment reserves, the settings of a primary frequency control system, the size and location of the disturbance, and the pre-disturbance operating conditions [21]. The frequency zenith represents the maximum drop/rise in frequency after a disturbance in a power system. The over- and under-frequency is problematic for system secure operation as it can trigger the protection systems and lead to load/generation disconnections. Therefore, frequency zenith is another key parameter to assess the stability performance of a power system subject to a certain control scheme. The frequency restoration control effectiveness represents the difference between the restored frequency and the nominal one and has to tend to 0, in order to prove the effectiveness of the control scheme. As proven in the simulations, the proposed KPIs represent a valuable tool for the frequency stability assessment in power system operation planning studies. Additionally, the flow of the whole process is shown in Figure 12. In more detail, the time step is set to the initial time stamp of the time-series data attached to system elements and then a load flow simulation is undertaken. Subsequently, an RMS simulation is performed during which a fault is imposed in one of the areas of the power network. The results are noted, and the time step is set to the next time moment to repeat the whole process. The simulations are repeated with and without the controllers for frequency regulation attached on distributed storage and the results obtained are statistically analyzed based on the defined KPIs.

**Table 3.** Key Performance Indices (KPIs).

	ID	Name	Formula
Key Performance Index	1	Frequency restoration control effectivity	$F_{restored} - F_{nom} \leq \varepsilon, \varepsilon \rightarrow 0$
	2	Frequency nadir	$\max(f_n - f) \text{ (Hz)}$ $f_{n,nominal} \text{ frequency (Hz)}$ $f_{system} \text{ frequency (Hz)}$
	3	Frequency zenith	$\min(f_n - f) \text{ (Hz)}$ $f_{n,nominal} \text{ frequency (Hz)}$ $f_{system} \text{ frequency (Hz)}$
	4	Rate of Change of Frequency (RoCoF)	$\frac{df}{dt} = \frac{P_g - P_l}{2H_{sys}}$ $\frac{df}{dt}$ —rate of change of frequency (Hz/s) $P_g$ —generators' active power (pu) $P_l$ —demand active power (pu) $H_{sys}$ —system inertia (s)
	5	Indication of Stability	Boolean variable (YES/NO)

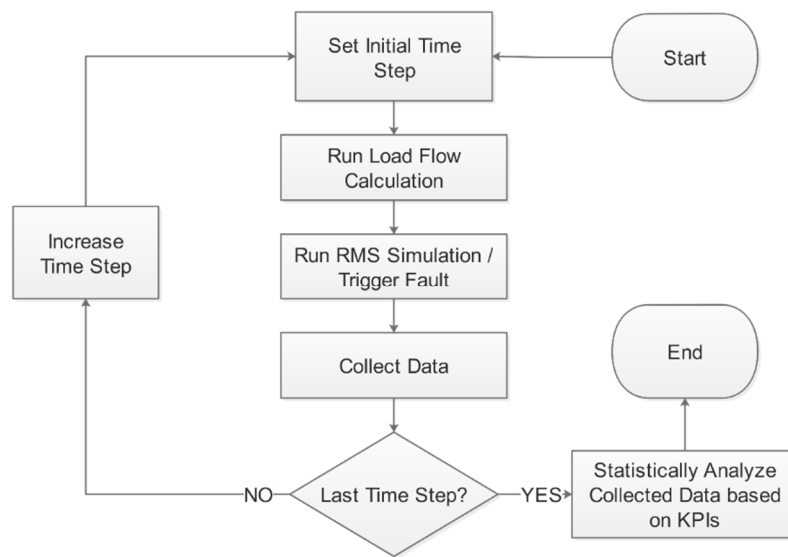


Figure 12. Flowchart for simulation/analysis process.

### 3. Simulation Case Results

From the simulations, it was observed that when significant loss of load/power generation occurs, frequency variation may become unstable. That is expected in systems with such high penetration of RES and thus low total inertia, especially when real events are simulated where a feeder with more than one resource may fail.

For the above reason, the frequency response and frequency stability will need to be controlled within the acceptable range by utilizing distributed generation resources and emerging technologies that provide flexibility and increase the resilience of the system. Advanced controllers need to be applied which will be able to manage the available power resource in a fast and effective manner to maintain frequency within nominal levels. It is expected that the controllers will be built in two hierarchical levels. The first will act locally within the area and the second hierarchical control level will allow the different areas to support each other for optimal operation. In this work, the higher-level controllers divide the frequency support effort onto the local area controllers attached on storage resources based on their nominal capacity. From the results for frequency variation presented in Figure 13, it is observed that the local control approach manages to minimize the frequency reduction effectively. It must be noted that the abbreviations shown in Figures 13–16 are referring to the studies cases as follows:

- A1—CD: Area No 1—Controllers Deactivated
- A1—CA: Area No 1—Controllers Activated
- A2—CD: Area No 2—Controllers Deactivated
- A2—CA: Area No 2—Controllers Activated
- PSA—CD: Power Station Area—Controllers Deactivated
- PSA—CA: Power Station Area—Controllers Activated
- WSA—CD: Wind Station Area—Controllers Deactivated
- WSA—CA: Wind Station Area—Controllers Activated

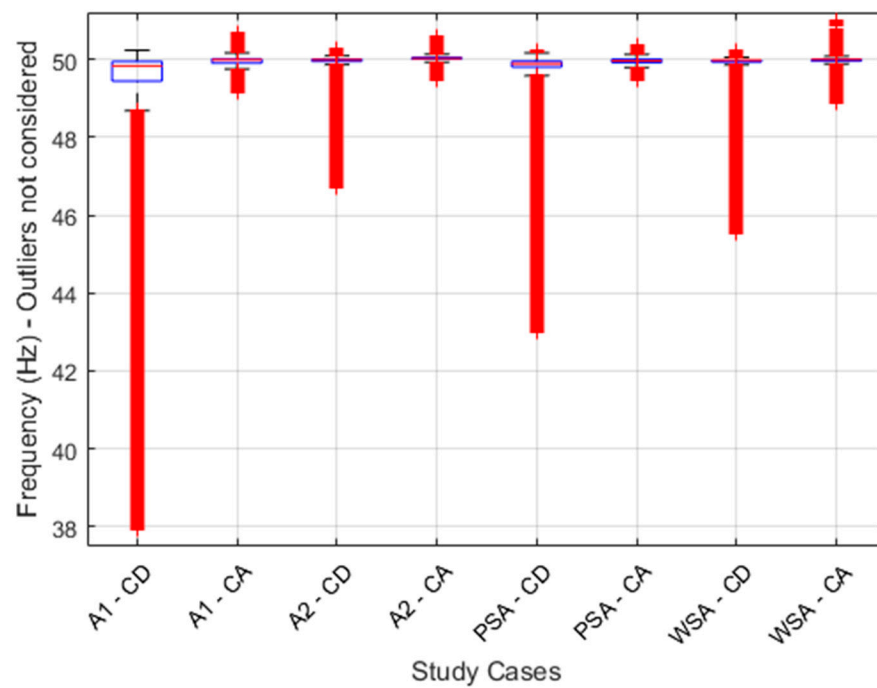


**Figure 13.** Frequency variation during the fault events with and without the controllers enabled (Box Plot Format)—All Study Cases.

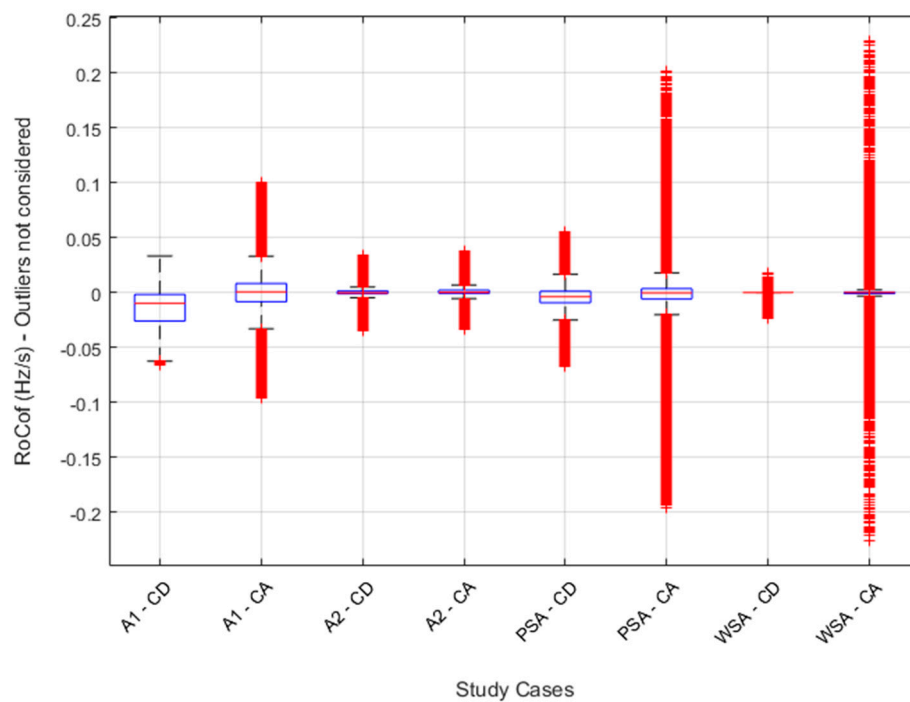


**Figure 14.** RoCoF variation during the fault events with and without the controllers enabled (Box Plot Format)—All Study Cases.

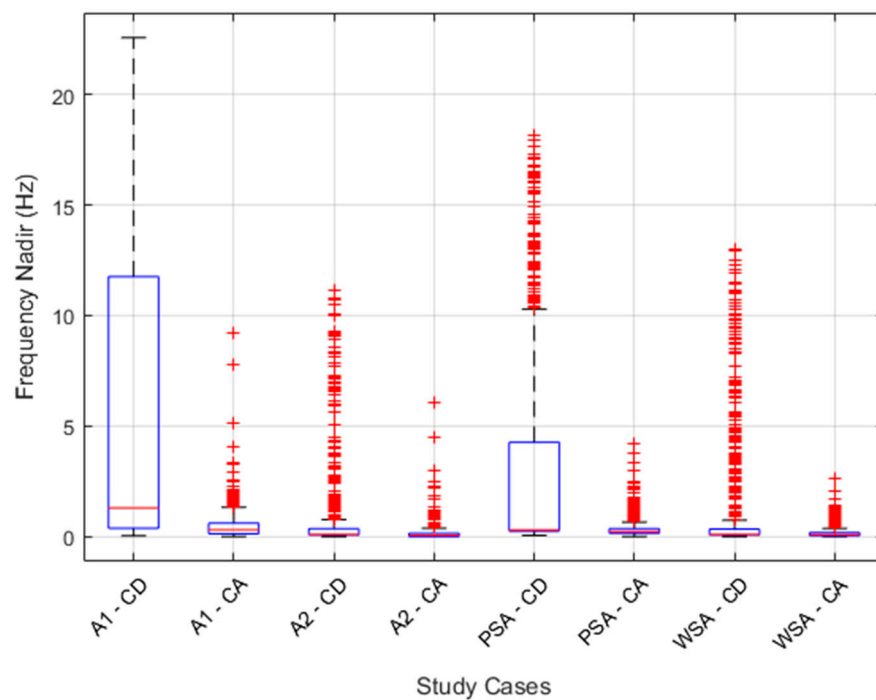


**Figure 15.** Frequency Nadir calculated with and without the controllers (Box Plot Format)—All Study Cases.

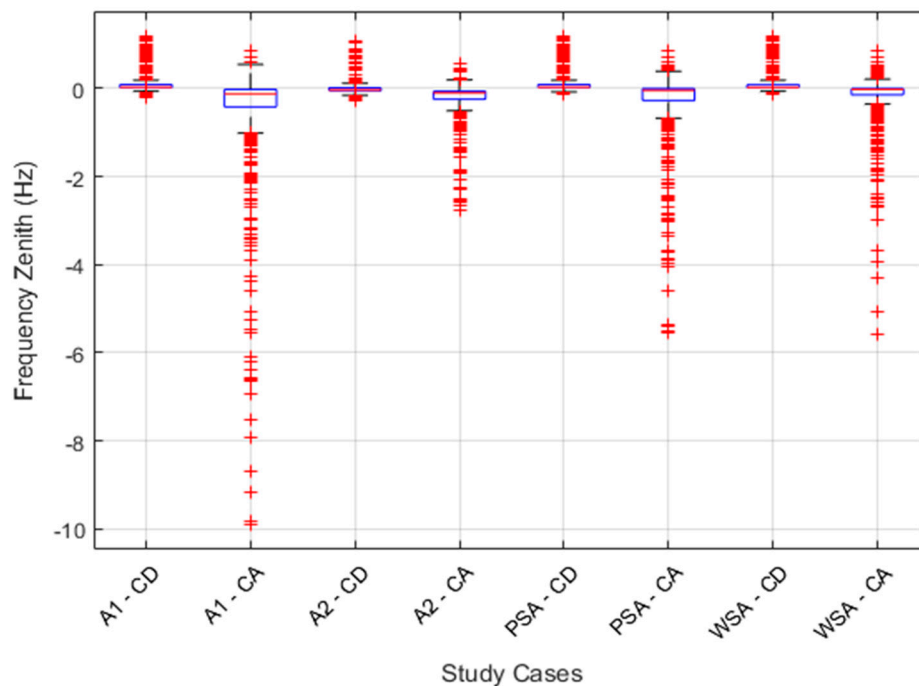


**Figure 16.** Frequency Zenith calculated with and without the controllers (Box Plot Format)—All Study Cases.

On the other hand, the steep frequency reduction is being avoided in most cases when the frequency regulation controls are enabled as lower negative values are observed in Figure 14. Additionally, in Figure 14 the controllers force the frequency to get into the acceptable range causing positive RoCoF values. In addition, the frequency nadir is being reduced significantly for all cases as depicted in Figure 15, but still they can cause considerable overshoot or oscillations in some situations if not tuned appropriately, as can be noticed in Figure 16.

As the study case of Area No. 1 fault has depicted the lower frequency values, it is chosen to present more detailed results about the specific study cases. The frequency variation of Area No. 1 fault is depicted in Figure 17. As can be seen in Figure 17, the frequency variation after the activation of the controller is reduced effectively in an acceptable range. During the event, it is obvious in Figure 18, that the controllers cause a positive response of RoCoF to force frequency within range.

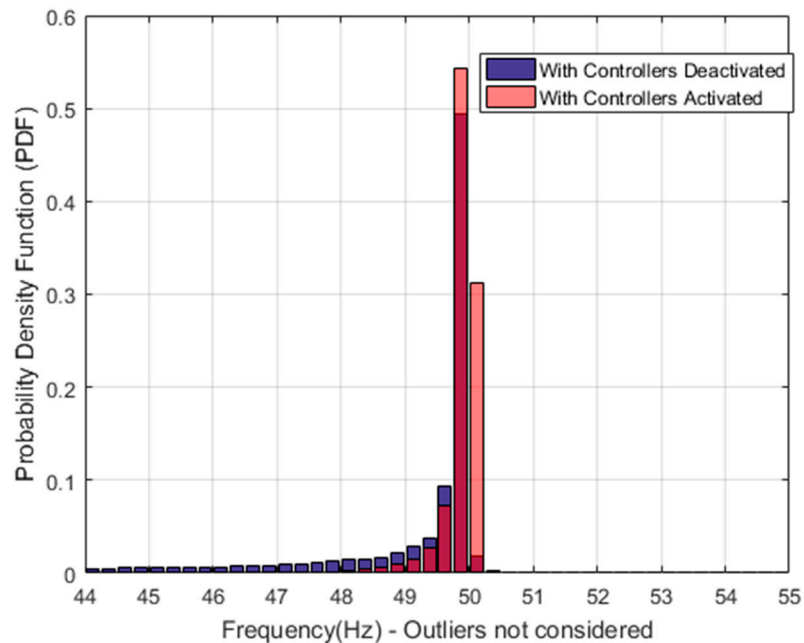


**Figure 17.** Frequency variation during the fault event with and without the controllers enabled (dark red is the combination of the two cases: with and without).

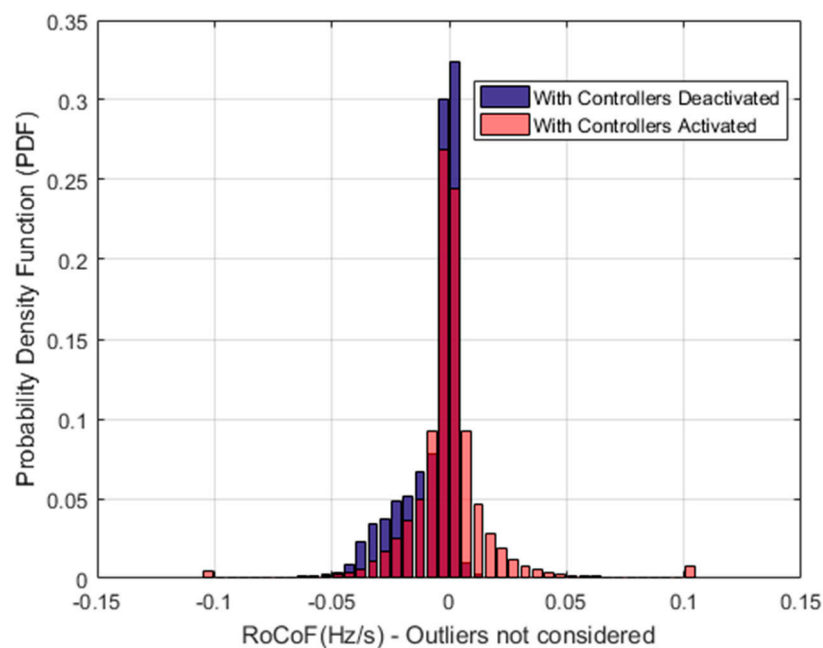


**Figure 18.** RoCoF variation during the fault event with and without the controllers enabled (dark red is the combination of the two cases: with and without).

From Figure 19 it is justified/verified that the controllers are quite effective in controlling frequency according to the target range. The frequency nadir of fault event is reduced as depicted in Figure 20 but in specific situations/event type the overshoot can be considerable (Figure 21) and controller must



be designed to handle it. In general, the overall frequency stability is improved by adopting controllers for frequency regulation as observed in Figure 22.

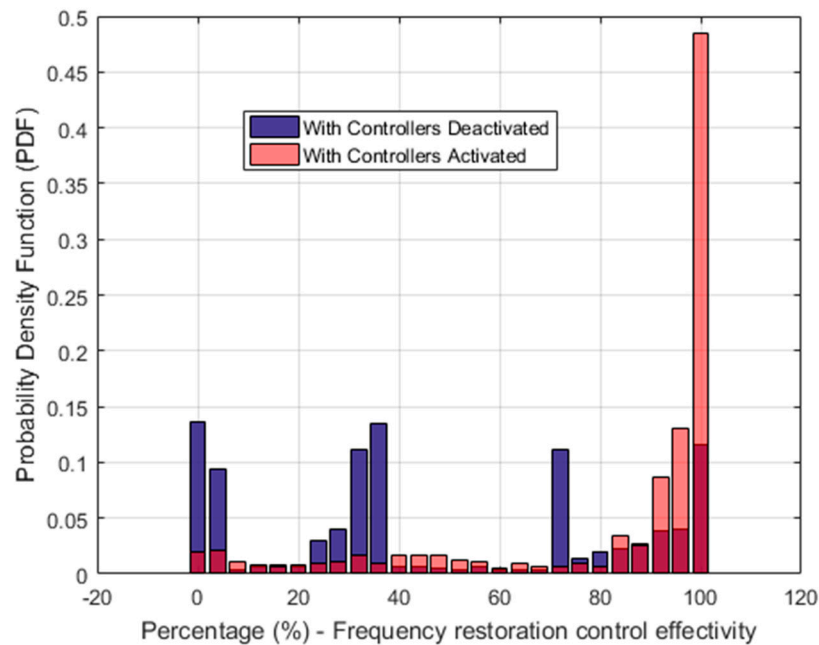


**Figure 19.** Control Effectiveness index with and without the controllers enabled (dark red is the combination of the two cases: with and without).

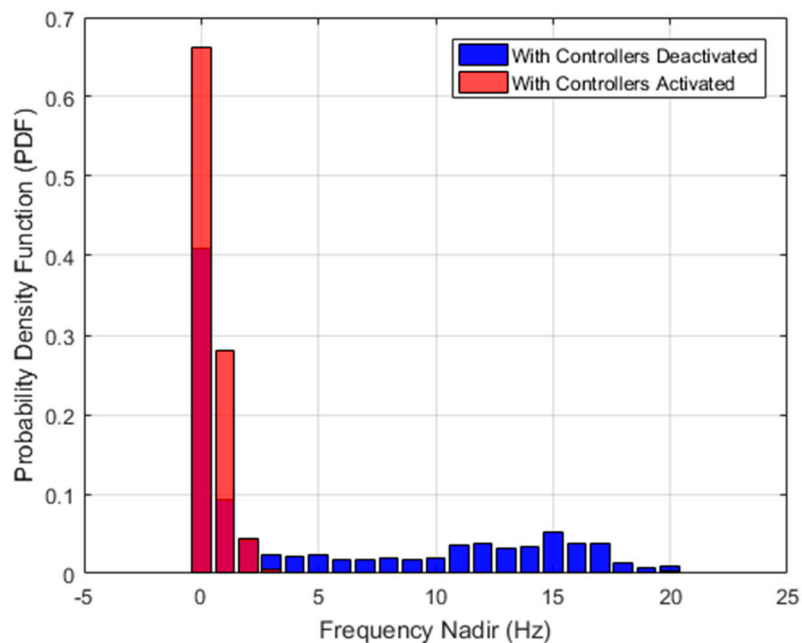


**Figure 20.** Frequency Nadir calculated with and without the controllers enabled (dark red is the combination of the two cases: with and without).

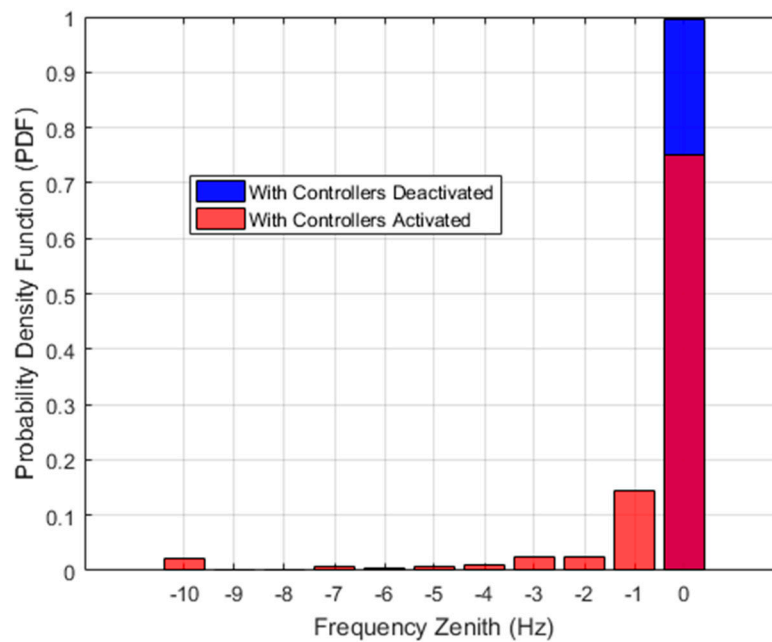


**Figure 21.** Frequency Zenith calculated with and without the controllers enabled (dark red is the combination of the two cases: with and without).

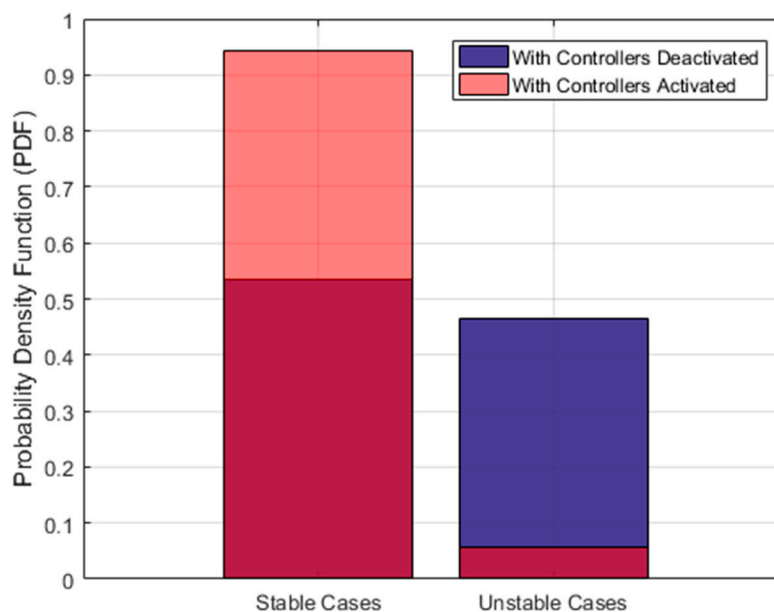


**Figure 22.** Stability Index calculated with and without the controllers enabled (dark red is the combination of the two cases: with and without).

#### 4. Discussion

The developed system of 2030 fully active down to the last distribution substations feeding active elements such as RES, storage, EVs, etc., is tested using the developed hierarchical controllers under different operational disturbances providing satisfactory results as follows:

- Results of frequency variation showing that the local control approach manages to minimize the frequency reduction effectively.
- The steep frequency reduction is being avoided in most cases when the frequency regulation controls are enabled as lower negative values are observed;
- The controllers force the frequency to get into the acceptable range causing positive RoCoF values;

- Justification/verification that the controllers are quite effective in controlling frequency according to the target range;
- The frequency nadir is being reduced significantly but still showing that considerable overshoots are still expected in some circumstances if not tuned appropriately;
- The overall stability is improved through the adaption of hierarchical controllers for frequency regulation;
- The hierarchical controllers are quite effective during severe events and can ever help in avoiding major or partial shutdown of the power grid;
- The hierarchical controllers must be a product of careful and meticulous design to be able to cope with all categories of events even with ones having low probability of occurrence.

Future research will focus on how FFR can be combined with inertia management to tackle holistically the low inertia challenge in the future grid operation, improve the intelligence of the controllers and extend them to cover the whole of the integrated grid.

## 5. Conclusions

The low inertia system of the future presents many operational challenges to handle, especially when disturbances occur throughout the system and frequency support and regulation is critical for the stability and the safety of the grid.

A major contribution of the paper is the introduction of hierarchical controllers capable of managing the active sources of the integrated grid thus improving system response under operational disturbances. A detailed presentation of the controllers used is included giving adequate details for the reader to appreciate the solvability objectives of the utilized concept.

This paper presents details of the adapted solutions, effectively tackling the identified challenge of low inertia systems, by providing

- A methodology for frequency stability evaluation of real systems;
- A true simulation of an active grid extending down to the distribution substation level;
- A two-level hierarchical control for effective Fast Frequency Control (FFR) including distributed local control;
- Utilization of the active sources of the grid down to the distribution substation level for frequency control/support, avoiding traditional operation schemes like underfrequency control schemes that are based on load rejection;
- A methodology for the evolution of the Cyprus grid system that is expected to be in operation in 2030 based on selected scenarios for the evolution of technologies and systems.

**Author Contributions:** Simulations, M.P.; Analysis of results, M.P. and C.N.P. and V.E.; Development of methodology, M.P. and C.N.P. and V.E.; Development of grid under test, M.P. and C.N.P. and V.E.; Implementation and evaluation of results, R.C. and M.D.S. and G.G. and M.V.; Design/Development of controller, A.W. and M.K. and R.C.; Literature review, A.W. and M.K.; Problem formulation, A.W. and M.K.; Research motivation. All authors have read and agreed to the published version of the manuscript.

**Funding:** This research was funded by European Union's Horizon 2020 Research and Innovation Programme grant number 773708.

**Acknowledgments:** The project INTERPLAN has received funding from the European Union's Horizon 2020 Research and Innovation Programme under Grant Agreement No. 773708.

**Conflicts of Interest:** The authors declare no conflict of interest.

## References

1. Union for the Coordination of Transmission of Electricity. *Operation Handbook Appendix 1—Load-Frequency Control and Performance*; ENTSO-E/UCTE: Paris, France, 2004. Available online: [www.entsoe.eu](http://www.entsoe.eu) (accessed on 8 May 2020).

2. ENTSO-E Technical Group on High Penetration of Power Electronic Interfaced Power Sources. *High Penetration of Power Electronic Interfaced Power Sources and the Potential Contribution of Grid Forming Converters*; Technical Report; ENTSO-E/UCTE: Brussels, Belgium, 2017. Available online: <https://euagenda.eu/upload/publications/untitled-292051-ea.pdf> (accessed on 8 May 2020).
3. Stenclik, D.; Richwine, M.; Miller, N.; Hong, L. The Role of Fast Frequency Response in Low Inertia Power Systems. In Proceedings of the CIGRE Technical Meeting, Paris, France, 26–31 August 2018.
4. O’connell, B.; Cuniffe, N.; Eager, M.; Cashman, D.; O’sullivan, J. Assessment of Technologies to Limit the Rate of Change of Grid Frequency on an Island System. In Proceedings of the CIGRE Technical Meeting, Paris, France, 26–31 August 2018.
5. Liu, Y.; You, S.; Liu, Y. Study of Wind and PV Frequency Control in U.S. Power Grids—EI and TI Case Studies. *IEEE Power Energy Technol. Syst. J.* **2017**, *4*, 1–9.
6. Thorbergsson, E.; Knap, V.; Swierczynski, M.; Stroe, D.; Teodorescu, R. Primary Frequency Regulation with Li-Ion Battery Based Energy Storage System—Evaluation and Comparison of Different Control Strategies. Intelec 2013. In Proceedings of the 35th International Telecommunications Energy Conference, Smart Power and Efficiency, Hamburg, Germany, 13–17 October 2013; pp. 1–6.
7. Sami, S.S.; Cheng, M.; Wu, J. Modelling and control of multi-type grid-scale energy storage for power system frequency response. In Proceedings of the 2016 IEEE 8th International Power Electronics and Motion Control Conference (IPEMC-ECCE Asia), Hefei, China, 22–26 May 2016; pp. 269–273.
8. Strassheim, A.; de Haan, J.E.S.; Gibescu, M.; Kling, W.L. Provision of frequency restoration reserves by possible energy storage systems in Germany and the Netherlands. In Proceedings of the 11th International Conference on the European Energy Market (EEM14), Krakow, Poland, 28–30 May 2014; pp. 1–5.
9. Hong, Q.; Nedd, M.; Norris, S.; Abdulhadi, I.; Karimi, M.; Terzija, V.; Marshall, B.; Bell, K.; Booth, C. Fast frequency response for effective frequency control in power systems with low inertia. *J. Eng.* **2019**, *2019*, 1696–1702. [CrossRef]
10. NERC (North American Electric Reliability Corporation). Inverter-Based Resource Performance Task Force (IRPTF) White Paper, March 2020. Available online: [https://www.nerc.com/comm/PC/InverterBased%20Resource%20Performance%20Task%20Force%20IRPT/Fast\\_Frequency\\_Response\\_Concepts\\_and\\_BPS\\_Reliability\\_Needs\\_White\\_Paper.pdf](https://www.nerc.com/comm/PC/InverterBased%20Resource%20Performance%20Task%20Force%20IRPT/Fast_Frequency_Response_Concepts_and_BPS_Reliability_Needs_White_Paper.pdf) (accessed on 8 May 2020).
11. Australian Energy Market Operator (AEMO). Fast Frequency Response in The Nem—Working Paper Future Power System Security Program, 2017. Available online: [https://www.aemo.com.au/-/media/Files/Electricity/NEM/Security\\_and\\_Reliability/Reports/2017/FFR-Working-Paper---Final.pdf](https://www.aemo.com.au/-/media/Files/Electricity/NEM/Security_and_Reliability/Reports/2017/FFR-Working-Paper---Final.pdf) (accessed on 8 May 2020).
12. Baghaee, H.R.; Mirsalim, M.; Gharehpetian, G.B.; Talebi, H.A. A Decentralized Power Management and Sliding Mode Control Strategy for Hybrid AC/DC Microgrids including Renewable Energy Resources. In *IEEE Transactions on Industrial Informatics*; IEEE: Piscataway, NJ, USA, 2017.
13. Baghaee, H.R.; Mirsalim, M.; Gharehpetian, G.B.; Talebi, H.A. Decentralized Sliding Mode Control of WG/PV/FC Microgrids under Unbalanced and Nonlinear Load Conditions for On- and Off-Grid Modes. *IEEE Syst. J.* **2018**, *12*, 3108–3119. [CrossRef]
14. Baghaee, H.R.; Mirsalim, M.; Gharehpetian, G.B.; Talebi, H.A. Nonlinear Load Sharing and Voltage Compensation of Microgrids Based on Harmonic Power-Flow Calculations Using Radial Basis Function Neural Networks. *IEEE Syst. J.* **2018**, *12*, 2749–2759. [CrossRef]
15. Baghaee, H.R.; Mirsalim, M.; Gharehpetian, G.B.; Talebi, H.A. A Decentralized Robust Mixed  $H_{\infty}/H_2$  Voltage Control Scheme to Improve Small/Large-Signal Stability and FRT Capability of Islanded Multi-DER Microgrid Considering Load Disturbances. *IEEE Syst. J.* **2018**, *12*, 2610–2621. [CrossRef]
16. Entso-e (The European Network for Transmission System Operators’ Electricity) Ten Year Development Plan (TYNDP) 2018 Public Report. Available online: [https://www.entso-g.eu/sites/default/files/files-old-website/publications/TYNDP/2018/entsos\\_tyndp\\_2018\\_Final\\_Scenario\\_Report\\_ANNEX\\_II\\_Methodology.pdf](https://www.entso-g.eu/sites/default/files/files-old-website/publications/TYNDP/2018/entsos_tyndp_2018_Final_Scenario_Report_ANNEX_II_Methodology.pdf) (accessed on 8 May 2020).
17. Cyprus’ Integrated National Energy and Climate Plan under the Regulation (EU) 2018/1999 of the European Parliament and of the Council of 11 December 2018 on the Governance of the Energy Union and Climate Action. Available online: [https://ec.europa.eu/energy/sites/ener/files/documents/cy\\_final\\_necp\\_main\\_en.pdf](https://ec.europa.eu/energy/sites/ener/files/documents/cy_final_necp_main_en.pdf) (accessed on 8 May 2020).
18. Bobinaite, V.; Di Somma, M.; Graditi, G.; Oleinikova, I. The Regulatory Framework for Market Transparency in Future Power Systems under the Web-of-Cells Concept. *Energies* **2019**, *12*, 880. [CrossRef]

19. Ciavarella, R.; Gradit, G.; Valenti, M.; Strasser, T.I. Innovative Frequency Controls for Intelligent Power Systems. In Proceedings of the 2018 International Symposium on Power Electronics, Electrical Drives, Automation and Motion (SPEEDAM), Amalfi, Italy, 20–22 June 2018; pp. 656–660.
20. ELECTRA IRP Project. *Simulations Based Evaluation of the ELECTRA WoC Solutions for Voltage and Balance Control—Stand-Alone Use Case Simulation Results*; WP 6, Control Schemes for the Use of Flexibility; ELECTRA Consortium, 2018.
21. Rakhshani, E.; Gusain, D.; Sewdien, V.; Torres, J.L.R.; Van Der Meijden, M.A. A Key Performance Indicator to Assess the Frequency Stability of Wind Generation Dominated Power System. *IEEE Access* **2019**, *7*, 130957–130969. [[CrossRef](#)]
22. Policy 1: Load-frequency control and performance, ENTSO-E, Continental Eur. Oper. Handbook, Tech. Rep., 2018. Available online: [https://www.entsoe.eu/\\_leadadmin/user\\_upload/\\_library/publications/entsoe/Operation\\_Handbook/Policy\\_1\\_\\_nal.pdf](https://www.entsoe.eu/_leadadmin/user_upload/_library/publications/entsoe/Operation_Handbook/Policy_1__nal.pdf) (accessed on 8 May 2020).
23. RG-CE System Protection & Dynamics Sub Group (REE, Terna, TransnetBW, 50Hertz Transmission, RTE, Swissgrid and Energinet.dk). *Frequency Stability Evaluation Criteria for the Synchronous Zone of Continental Europe*; ENTSO-E: Brussels, Belgium, 2016.



© 2020 by the authors. Licensee MDPI, Basel, Switzerland. This article is an open access article distributed under the terms and conditions of the Creative Commons Attribution (CC BY) license (<http://creativecommons.org/licenses/by/4.0/>).